catalysts

MDPI

Article

Selective Hydrogenation of Acetylene over Pd-Mn/Al_2O_3 Catalysts

Dmitry Melnikov *, Valentine Stytsenko, Elena Saveleva, Mikhail Kotelev, Valentina Lyubimenko, Evgenii Ivanov, Aleksandr Glotov and Vladimir Vinokurov

Physical and Colloid Chemistry Department, Gubkin Russian State University of Oil and Gas, 65 Leninsky prosp, 119991 Moscow, Russia; vds41@mail.ru (V.S.); savel0394@gmail.com (E.S.); kain@inbox.ru (M.K.); ljubimenko@mail.ru (V.L.); ivanov166@list.ru (E.I.); glotov.a@gubkin.ru (A.G.); vinok_ac@mail.ru (V.V.)

* Correspondence: melnikov.dp@mail.ru

Received: 17 April 2020; Accepted: 2 June 2020; Published: 4 June 2020

Abstract: Novel bimetallic Pd-Mn/Al_2O_3 catalysts are designed by the decomposition of cyclopentadienylmanganese tricarbonyl (cymantrene) on reduced Pd/Al_2O_3 in an H_2 atmosphere. The peculiarities of cymantrene decomposition on palladium and, thus, the formation of bimetallic Pd-Mn catalysts are studied. The catalysts are characterized by N_2 adsorption, H_2 pulse chemisorption, temperature-programmed desorption of hydrogen (TPD-H_2), transmission electron microscopy (TEM), energy-dispersive X-ray spectroscopy (EDX), X-ray diffraction (XRD), and diffuse reflectance infrared Fourier transform spectroscopy (DRIFTS). The modified catalysts show the changed hydrogen chemisorption properties and the absence of weakly bonded hydrogen. Using an organomanganese precursor provides an uniform Mn distribution on the catalyst surface. Tested in hydrogenation of acetylene, the catalysts show both higher activity and selectivity to ethylene (20% higher) compared to the non-modified Pd/Al_2O_3 catalyst. The influence of the addition of Mn and temperature treatment on catalyst performance is studied. The optimal Mn content and treatment temperature are found. It is established that modification with Mn changes the route of acetylene hydrogenation from a consecutive scheme for Pd/Al_2O_3 to parallel one for the Pd-Mn samples. The reaction rate shows zero overall order by reagents for all tested catalysts.

Keywords: acetylene hydrogenation; ethylene production; bimetallic catalysts; palladium; manganese; cymantrene

1. Introduction

Ethylene is one of the commonly used monomers in the petrochemical industry worldwide and is produced by the steam cracking of hydrocarbons. Ethylene cuts typically comprise 0.5%–2% of acetylene, which is a poison for the polymerization catalysts and should be removed by selective hydrogenation to ethylene [1]. A number of active metals (Pd, Ni, Au) modified with a wide range of elements (Ag, Cu, Si, Ga, Sn, Pb, In, S, Fe) and supported on various carriers (Al_2O_3, SiO_2, TiO_2, ZnO) were investigated [2–25].

Monometallic Pd catalysts show a high activity but low selectivity to ethylene, so Pd is typically promoted with other metals. In industry, Pd-Ag/Al_2O_3 catalysts are widely used and much research is devoted to Pd-Ag compositions supported on alumina or silica. It is supposed that the promotion is based on an increased electronic density of the Pd *d*-band resulting in a decrease in ethylene [3] or hydrogen adsorption with further spill over [4]. In addition, it is suggested that the promotion is caused by not only an electronic but also a geometric effect [5], or just geometric [8]. Pd-Ag catalysts expose not only a higher selectivity to ethylene, but also a lower yield of C_{6+} hydrocarbons (green oil)

as compared to Pd/Al_2O_3, which is crucial for the cycle length of the catalysts [9]. However, problems with the deactivation of Pd-Ag catalysts during the selective hydrogenation of acetylene are as actual as before [8]. The main drawback of promotion with Ag is the significant reduction in catalyst activity—about 20 times as low as pure Pd [12]. Pure nickel shows a lower selectivity than even pure Pd, but the addition of Zn (such as $Ni\text{-}Zn/MgAl_2O_4$) increases the selectivity to the level of Pd-Ag catalysts [17] and decreases oligomerization [26].

Besides Ag, a number of other metals were investigated as promotors. The addition of Ga leads to an increased selectivity (71% at 99% conversion) compared to Pd catalysts, but also with Pd-Ag (49% at 83% conversion) [11–13]. The increased selectivity is explained by the isolation of the Pd sites [11,12] and the additional modification of the Fermi level of palladium [13]. The activity of Pd-Ga catalysts is similar to that of Pd-Ag.

Palladium modification with Cu shows a benefit in selectivity compared to $Pd\text{-}Ag/Al_2O_3$ [15,16] only when it is provided by the surface redox method, which is explained by blocking low coordinated Pd atoms (responsible for the low selectivity to ethylene) and by the hydrogenation properties of copper. Pure copper, however, requires significantly higher operating temperatures and shows an unacceptably high oligomer yield (up to 40%) [19].

A Pd-Zn catalyst supported on carbon or Al_2O_3 also shows a higher selectivity (+20%–50%) compared to pure palladium [20,21]. It was previously proved that Pd and Zn form a nanoalloy [27]. Moreover, Zn decreases the acidity of support and, hence, green oil formation.

As the carriers for hydrogenation catalysts, natural clay nanotubes such as halloysite are of particular interest [28–30]. Halloysite has the appropriate surface area (50–300 $m^2.g^{-1}$), a high ion-exchange capacity, and a micro-mesoporous structure that enables the synthesis of highly active catalysts and new materials applied for heterogeneous catalytic systems. Thus, a new approach was developed—a self-assembling synthesis of structured mesoporous silica on clay nanotubes (HNT), which was applied to create the highly porous material MCM-41-HNT with an enhanced thermal and mechanical stability [31].

Hard reducible oxides, such as Ce, Ti, and Nb, are also investigated as promotors [32,33]. The most efficient was TiO_2, however the catalyst selectivity did not exceed 50% at 90% conversion. The promotion effect is explained by the geometric and electronic modification of the Pd surface.

Supported on glass nanofibers, Pd also shows a high selectivity (up to ~56% at total conversion) [34,35]. The high selectivity is explained by: 1) the stabilized small Pd particles (~1 nm) in the subsurface of the glass fibers and 2) the much higher adsorption ability of acetylene compared to ethylene on Pd inside a glass matrix. As a result, the hydrogenation of ethylene from the gas phase is actually absent. Besides palladium, another interesting active metal in acetylene hydrogenation is gold. It is reported that Au/Al_2O_3 shows 100% selectivity at temperatures of 313–523 K, because ethylene hydrogenation only starts at temperatures above 573 K [23]. A lower selectivity was achieved on Au/TiO_2 (90% at 88% conversion). $Au\text{-}Pd/TiO_2$ catalysts show a higher activity compared to Au/TiO_2, but their selectivity is lower [24].

The addition of iron in the form of Fe^0 to Pd increases the selectivity to the olefin in the hydrogenation of both acetylene (88% at 87% conversion) [22] and phenylacetylene (90% at 99% conversion) [36,37].

The preparation of bimetallic catalysts (BMC) comprising VIII group metals by the decomposition of organometallic compounds has been patented [38–40] and reviewed in [41]. The decomposition of organometallic species under reduction conditions enables an easy formation of bimetallic catalysts with a zero valence state of the second metal. Some examples of BMC having unusual properties are as follows: Rh-Sn (butyl) [42], Pd-Pb (butyl) [43], Ni-Cr (arene) [44], and Pd-Fe (ferrocene) [22].

In this study, a number of $Pd\text{-}Mn/Al_2O_3$ catalysts were prepared by the decomposition of cymantrene on a reduced Pd/Al_2O_3 precursor. The use of cymantrene has some peculiarities as the molecule contains two types of ligands: CO and cyclopentadienyl. The catalysts were tested in a selective hydrogenation of acetylene. In all cases, Mn increases the catalyst's selectivity to ethylene as

compared with the Pd/Al_2O_3 sample. Moreover, the Mn-modified samples have shown higher activity. It is found that the addition of Mn suppresses the hydrogen chemisorption on Pd catalysts.

2. Results and Discussion

2.1. Cymantrene Decomposition on Pd/Al_2O_3

To investigate the formation of $Pd\text{-}Mn/Al_2O_3$ catalysts, the decomposition of cymantrene on Pd/Al_2O_3 was performed in a temperature-programmed regime in an H_2 flow with a mass spectrometry analysis of effluent gas. Figure 1 shows the mass-spectra of cymantrene decomposition products in the range of 40–400 °C.

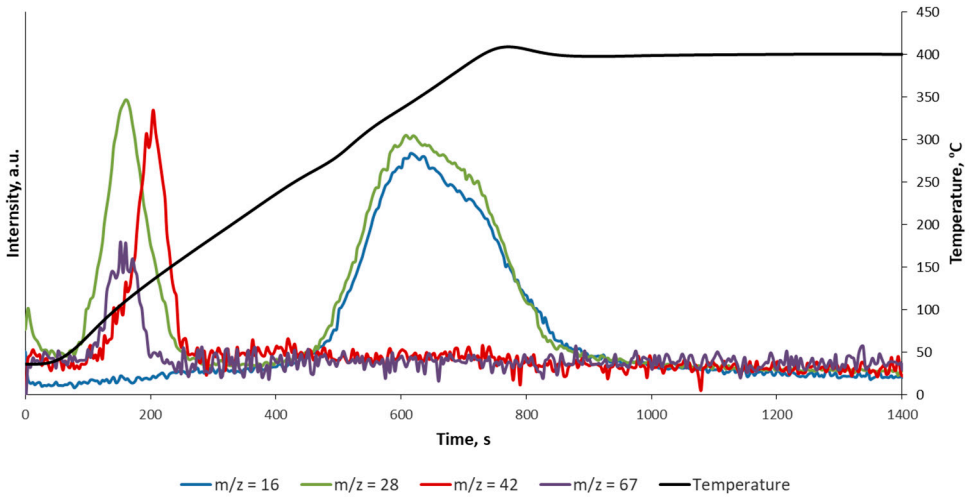

Figure 1. Decomposition of cymantrene on $0.068\%Pd/Al_2O_3$ in H_2 flow at temperatures of 40–400 °C.

As shown, at the initial step (temperatures of 80–150 °C) there are peaks with m/z 28 (carbon monoxide), 42 (cyclopentane), and 67 (cyclopentene) [45]. In the temperature range of 270–400 °C, one can observe two peaks with m/z 16 (methane) and 28 (carbon monoxide). The peaks corresponding to cyclopentadiene (m/z 65, 66) are absent. More details about the mass spectra interpretation are shown in the Supplementary Materials.

We may conclude, therefore, that the cyclopentadienyl ligand of cymantrene is removed after hydrogenation, mainly as cyclopentane at 80–150 °C. As for carbon monoxide, it is strongly bonded with metals, and may be removed as methane at temperatures above 270 °C [46]. However, as evidenced by the mass-spectrometric analysis of the effluent gas, to complete a CO removal a treatment in an H_2 flow at 400 °C for 10 min is necessary.

2.2. Catalysts Characterization

Table 1 summarizes the properties of the prepared catalysts. The designation of the samples shows the atomic Mn/Pd ratio and the treatment temperature, which is the final temperature of the cymantrene decomposition. As Table 1 shows, the Brunauer–Emmett–Teller (BET) surface area of the samples is the same within the margin of error, which indicates that the addition of Mn has no significant effect on the surface area of the catalysts. However, the samples show quite a different behavior in H_2 chemisorption.

Table 1. Physicochemical data of alumina supported catalysts.

Sample	Catalyst Composition [1]	Hydrogen Treatment Temperature, °C	BET Surface Area, m^2/g	H_2 Adsorption, µmol/g cat	Selectivity to Ethylene [2] at 40 °C, %
Pd-250	0.068%Pd	250	133	1.20	70
PdMn-1-250	0.068%Pd-0.029%Mn	250	133	0.18	91
PdMn-1-330	0.068%Pd-0.029%Mn	330	131	1.10	80
PdMn-2-300	0.068%Pd-0.063%Mn	300	129	0.03	92
PdMn-2-350	0.068%Pd-0.063%Mn	350	128	0.04	89

[1] Hereafter, all catalyst compositions are in wt. %, [2] Acetylene conversion is 60%.

The non-promoted Pd/Al_2O_3 catalyst uptakes a significant amount of H_2 (1.2 µmol/g), but any addition of Mn decreases the H_2 adsorption. For example, an addition of 0.029% Mn (PdMn-1-250 and PdMn-1-330) decreases the H_2 adsorption to 1.1 µmol/g (for the sample treated at 330 °C) and to 0.18 µmol/g (for the sample treated at 250 °C). This trend is enhanced by a further addition of Mn: both PdMn-2-300 and PdMn-2-350 uptake significantly less H_2 (0.03 and 0.04 µmol/g). It should be noted that there are two possible reasons for the decreasing H_2 adsorption: the shielding of Pd with Mn atoms and the blocking of H_2 adsorption sites by residual CO ligands. Moreover, the selectivity of Pd-Mn catalysts to ethylene is correlated with their H_2 adsorption, as shown in Table 1.

As depicted in Figure 2, the non-modified Pd-250 desorbs H_2 in the range of 80–250 °C, indicating a desorption of weakly bonded hydrogen at low temperatures and strongly bonded hydrogen (or Pd hydride decomposition) at a temperature ramp.

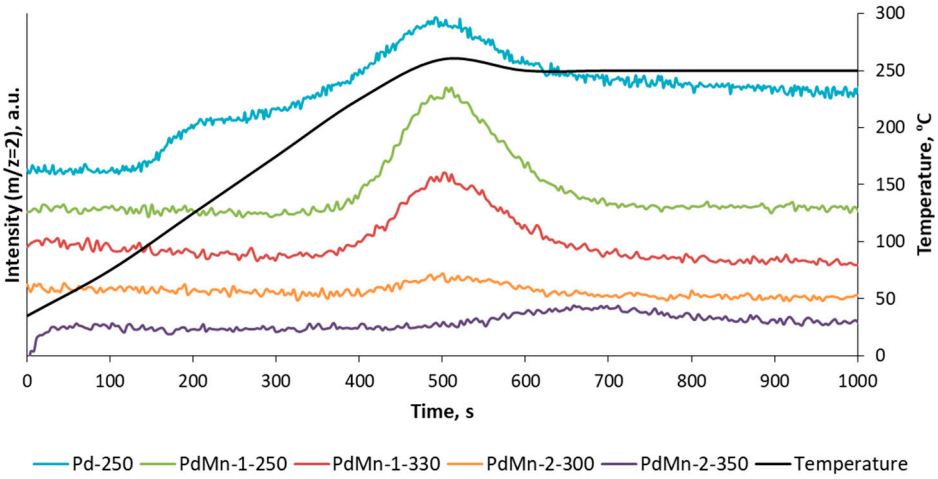

Figure 2. TPD-H_2 spectra of the samples.

The samples with a low Mn content (PdMn-1-250 and PdMn-1-330) do not desorb H_2 at temperatures below 230 °C, which indicates the presence of strongly bonded hydrogen (or Pd hydride). The samples (PdMn-2-300 and PdMn-2-350) with a high Mn content demonstrate only an insignificant H_2 desorption at a temperature of 250 °C, and these findings correlate with the chemisorption data (Table 1). Decreasing strongly chemisorbed hydrogen is recommended for acetylene selective hydrogenation as reported in [4,25,47].

As depicted on the TEM images of the PdMn-2-300, Pd nanoparticles (NP) with a lattice spacing of about 0.228 nm are found, which are indexed as the (111) plane for cubic palladium doped with clusters from single Mn atoms (Figure 3a) and Mn crystallites (Figure 3b) [48,49]. Depending on the lattice spacing, the fringes on the TEM images could be assigned to Pd nanoparticles or Mn crystallites and in some cases to manganese oxides with a lattice spacing of about 0.47–0.49 nm [49,50]. Due to the overlapping of Mn crystallites on Pd NPs, it is difficult to measure accurately the palladium

nanoparticles' size and their distributions [51], but TEM images show Pd NPs in the range of 5–10 nm with a mean particle size of about 6.7 ± 0.2 nm (Figure 3c), in agreement with the literature data [48].

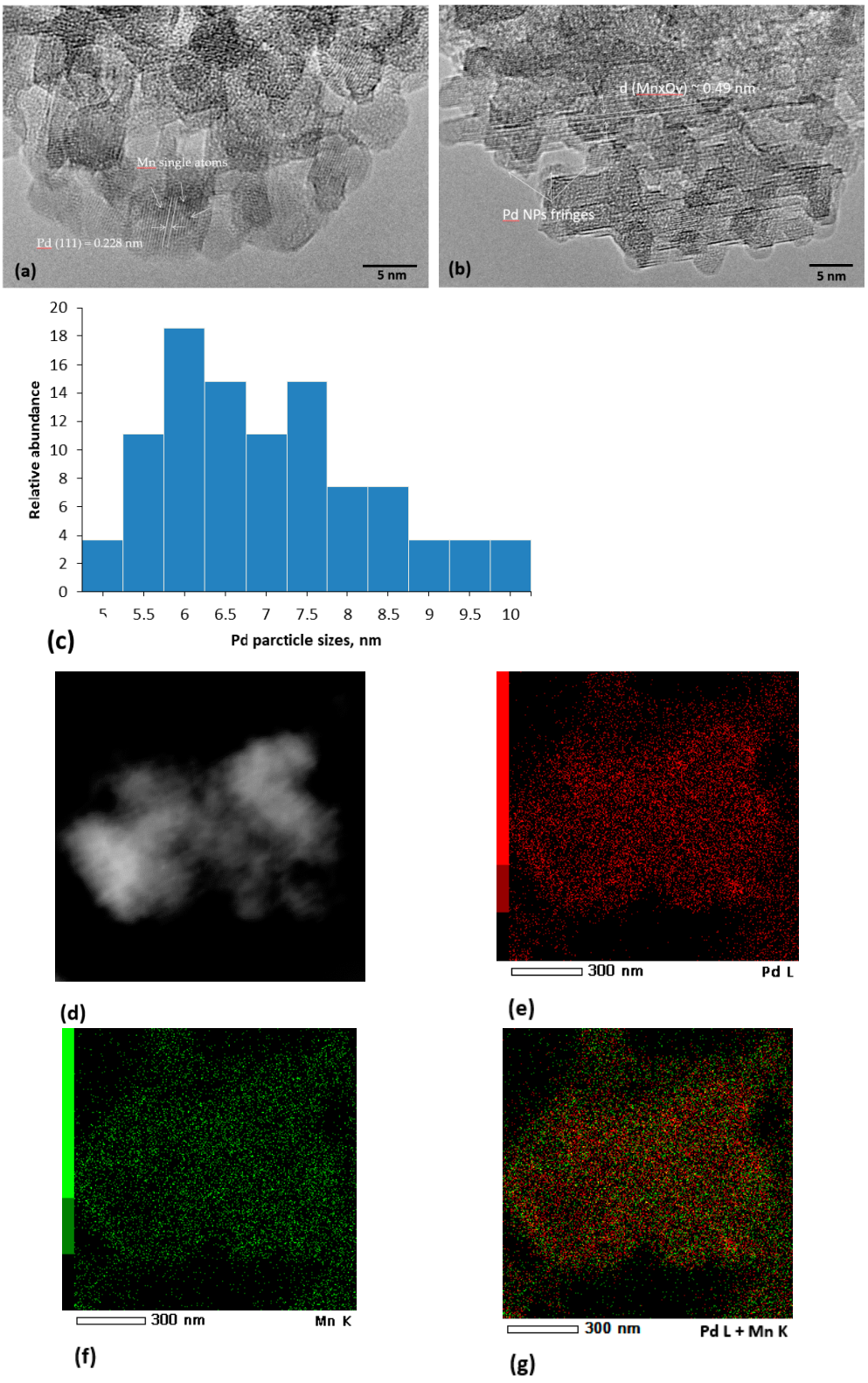

Figure 3. TEM imaging of the sample 4: (**a**,**b**) TEM image; (**c**) particle size distribution; (**d**) STEM image; (**e**) Pd mapping (L line); (**f**) Mn mapping (K line); (**g**) Pd (L) + Mn (K) mapping overlay.

Figure 3d–f show a STEM image and its EDX mapping of PdMn-2-300. It is clear that Pd and Mn are uniformly distributed over the alumina support with high dispersion. As shown in Figure 3g, both metals are in close contact.

XRD found no reflections, which could be related to Pd and Mn due to the low metal content, as Figure 4 shows.

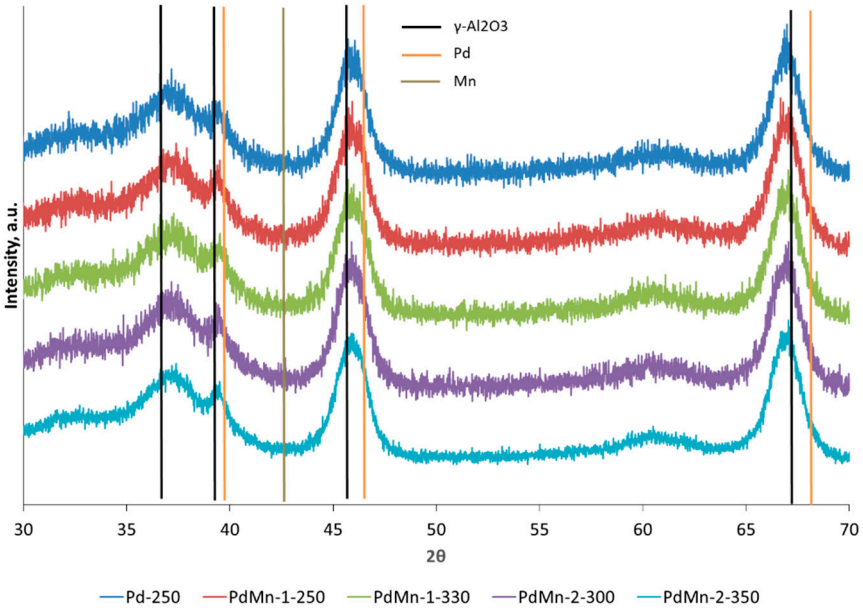

Figure 4. XRD patterns of Pd-Mn/Al_2O_3 samples.

Additional information about the chemisorption properties of the catalysts is obtained using DRIFT spectroscopy of PdMn-1-330. Figure 5 shows two spectra of the catalyst samples. For the first measurement, one sample is just treated in a vacuum for 2 h. For the second measurement, another sample is preliminarily treated with H_2 at 250 °C (30 min), acetylene at 20 °C (10 min), and H_2 at 20 °C (10 min) with a final purge with Ar at 20 °C (10 min) and treated in a vacuum for 2 h.

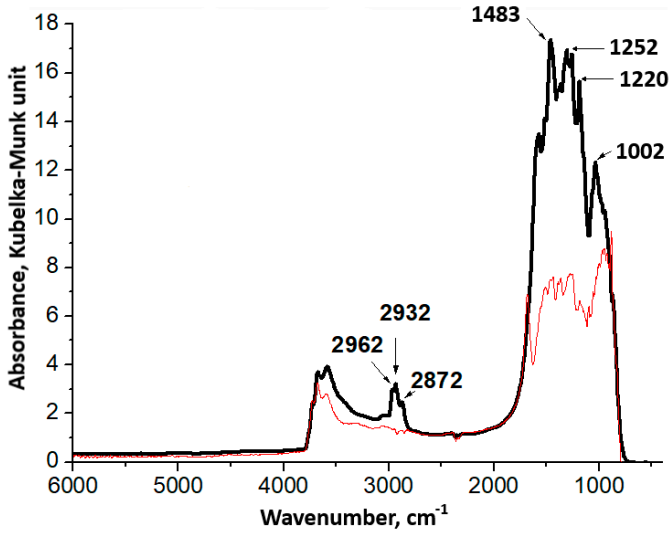

Figure 5. Diffuse reflectance infrared Fourier transform spectroscopy (DRIFTS) spectra of PdMn-1-330 without pretreatment (red line) and treated with C_2H_2 and H_2 (black line).

As the spectra show, there are two regions: 2500–3800 cm^{-1}, which corresponds to the vibrational spectra of O–H and C–H bonds, and 700–2400 cm^{-1}, ascribed to the vibrational spectra of Al_2O_3,

adsorbed water, carbonyls, and others [52]. After the pretreatment, seven additional bands are observed: 2962, 2932, 2872, 1483, 1252, 1220, and 1002 cm^{-1}. The bands 2962, 2932, and 2872 cm^{-1} may be ascribed to C–H stretching in the C_2H_6 molecule [53] and the bands 1220 and 1252 cm^{-1} to vibrations of C–C bonds in the C_2H_2 molecule [54]. The band 1002 cm^{-1} may be assigned to C=C bending in the C_2H_4 [53]. It should be stressed that all bands above are observed only after the treatment of PdMn-1-330 with C_2H_2. After vacuum treatment of the sample (2 h, 200 °C), the intensity of the spectra in the region of 2962–2872 cm^{-1} decreases slightly, which points out the strong chemisorption of the species above.

The DRIFT spectra of adsorbed CO are considered in the Supplementary Materials.

As shown by the DRIFT, the CO adsorption over the Pd-Mn catalysts was weak and negligible (at most 0.015 units Kubelka-Munk). After the vacuum treatment at room temperature, all peaks in the range of 2195–1871 cm^{-1} disappeared. So, one may conclude that there is an absence of strong CO chemisorption on the catalysts.

2.3. Catalytic Tests

Figure 6a shows the conversion of acetylene (X) as a function of the contact time (t) for the samples at 40 °C. For all of the Mn-promoted catalysts, the conversion values are at the same level (within the margin of error), regardless of the Mn addition and treating temperature. Moreover, at a given contact time, the Mn-promoted samples provide a significantly higher conversion (~20%) compared to that of Pd-250. The linear form of X(t) lines indicates the overall zero order by reagents.

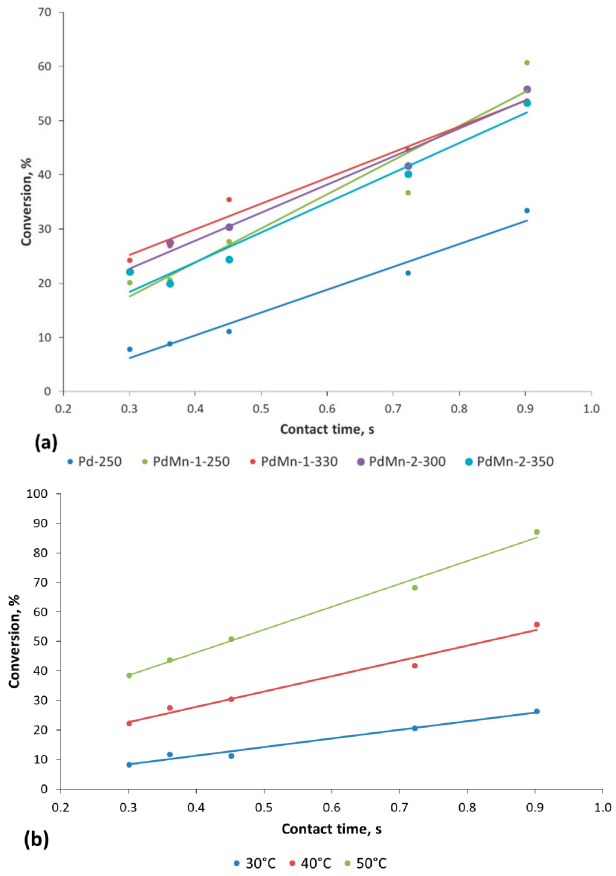

Figure 6. Acetylene conversion vs. contact time: (**a**) for the Pd-Mn/Al_2O_3 catalysts; (**b**) for PdMn-2-300 at 30, 40, and 50 °C.

Based on these experimental data and taking into account the selectivity obtained (Figure 7), we may consider a mass ratio of Mn/Pd ~ 1 (atomic ratio Mn/Pd ~ 2) and a treatment temperature of 300 °C for 30 min as optimal, corresponding to the PdMn-2-300 sample.

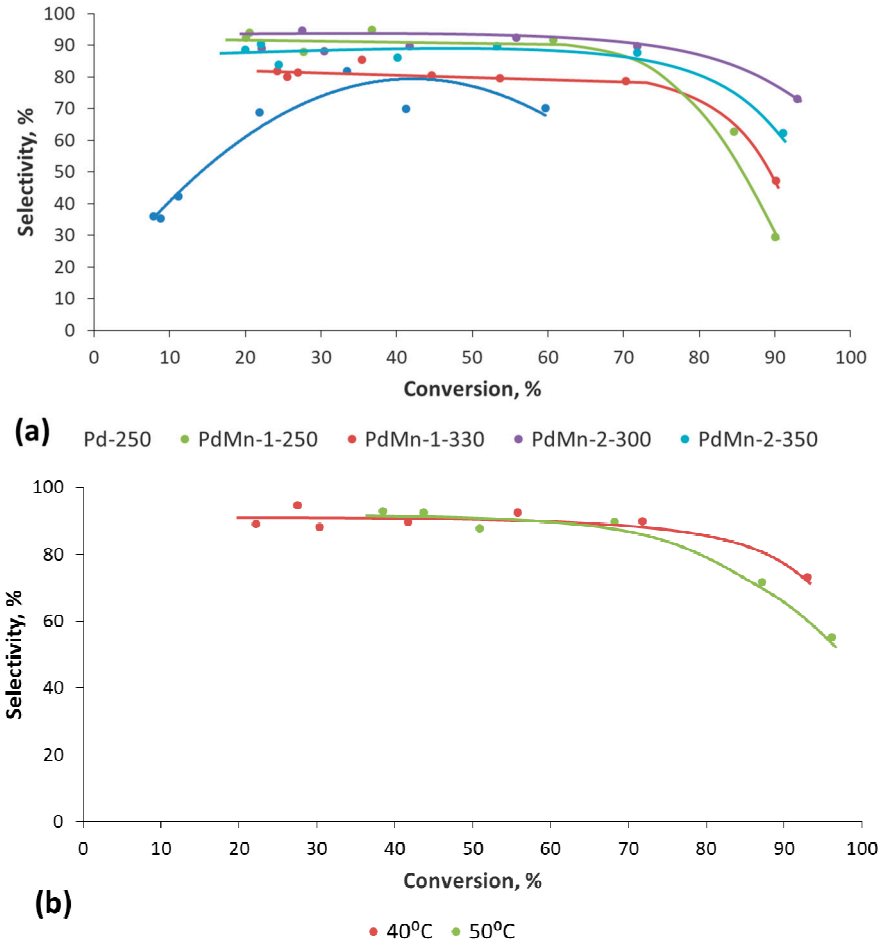

Figure 7. Ethylene selectivity vs. conversion at 40 °C for alumina-supported Pd-Mn catalysts: (**a**) effect of treatment temperature and Mn content; (**b**) PdMn-2-300 at 40 and 50 °C.

Figure 6b shows the conversion vs. contact time for PdMn-2-300 at 30, 40, and 50 °C. At all temperatures, the X(t) lines are straight, so the zero order by reagents is kept.

Figure 7 shows the selectivity to ethylene on the conversion for all samples at 40 °C. For Pd-250, the selectivity is the lowest and the curve has a maximum, which is typical in the case of a consecutive scheme of acetylene hydrogenation to ethylene and ethane:

$$C_2H_2 \rightarrow C_2H_4 \rightarrow C_2H_6 \quad (1)$$

in accordance with [55].

However, Mn-containing samples maintain a selectivity at a level of 80%–92% up to acetylene conversions of more than 70%, which implies the parallel scheme of acetylene hydrogenation to ethylene and ethane:

$$C_2H_6 \leftarrow C_2H_2 \rightarrow C_2H_4 \quad (2)$$

as previously observed on Pd-Fe/Al_2O_3 catalysts [22]. The PdMn-1-250 sample shows a selectivity of ~ 91% at a conversion of below 70%. Increasing the treating temperature to 330 °C (PdMn-1-330), and thus eliminating the strongly chemisorbed CO ligands, decreases the selectivity to ~80% at the same conversions.

Both samples with high Mn contents show a better selectivity at high conversions. The most selective is PdMn-2-300, of which the selectivity is ~92% in the conversion range of below 70%. The result is in accordance with the data published [56], where a catalyst having an Mn/Pd atomic ratio of two provides the highest selectivity to 1,3-butadiene in vinylacetylene hydrogenation.

Figure 7b shows the influence of the reaction temperature on the S(X) curve for PdMn-2-300 at 40 and 50 °C. It is obvious that the selectivity is the same (~90%) up to a conversion of ~70% irrespective of the temperature, which indicates that the activation energies of both reaction routes in scheme two are very close.

Our catalyst advantages are illustrated in Table 2, comprising the characteristics of the best Pd-containing catalysts in acetylene hydrogenation.

Table 2. Comparative characteristics of the best Pd-containing catalysts in acetylene hydrogenation.

Article	Catalyst	T, K	P, bar	X, %	S, %	Activity, mol/g Pd/h	TOF (Turnover Frequency), s^{-1}
[12]	$Pd_{30}Ga_{70}$	473	1	99	71	0.012 [1]	-
[24]	Pd-Au/TiO_2	343	1	100	45	~0.283 [2]	-
[25]	Pd-In/Al_2O_3	333	21	~85	~40	-	0.8
[35]	Pd/Fiberglass	328	1	80	60	-	0.55
[8]	$Pd_{20}Ag_{80}/Al_2O_3$	303	10	67	72	-	0.5
[22]	Pd-Fe/Al_2O_3	318	1	87	88	1.67	0.31
This work	PdMn-2-300	313	1	87	81	4.22	0.74

[1] Recalculated from g/g cat/h, [2] Calculated by authors using data [24]: acetylene concentration and conversion, GHSV, Pd content and Pd density.

As Table 2 shows, the catalysts developed are of the same order of activity (in terms of turnover frequency (TOF)) but exceed the known one in ethylene yield (the product of X and S, calculated by acetylene (defficiency) conversion without hydrogen (excess)) and molar activity under mild conditions.

One may conclude, therefore, that modification with manganese improves both the activity (in terms of mol/g_{Pd}/h) and selectivity of palladium catalysts in acetylene hydrogenation.

For qualitative evaluation of the catalyst stability on a laboratory scale, the selectivity to the C_4 compound (namely, 1,3-butadiene as an initial dimerization product of the acetylenic species [9]) is used, which is a fundamental indicator of the palladium-containing catalyst stability in the selective hydrogenation of acetylene [8]. The absence of C_4 hydrocarbons is confirmed by GC and MS-analyses for all set experiments performed. More details about the analyses and the stability of the catalysts are shown in the Supplementary Materials. Based on the evidence above, we consider the Pd-Mn/Al_2O_3 catalysts to be stable for at least 5 h.

3. Materials and Methods

3.1. Chemical Reagents

Microspherical γ-Al_2O_3—SKTB Katalizator (Novosibirsk, Russia); cymantrene-cyclopentadienylmanganese tricarbonyl or $(CO)_3$Mn-(cyclo-C_5H_5) (Sigma-Aldrich, St. Louis, MO, USA); $PdCl_2$—Aurat (Moscow, Russia); Ar (99,993%), H_2 (99,99%), He (99,995%), C_2H_2 (99,1%), C_2H_4 (99,9%)—NII KM (Moscow, Russia); $NH_3 \cdot H_2O$ (~25%)—ECOS-1 (Moscow, Russia).

3.2. Catalysts Preparation

The initial catalyst 0.068% Pd/Al_2O_3 was prepared by a wet impregnation of γ-Al_2O_3 (preliminary calcined for 3 h at 600 °C) with an aqueous ammonia solution of $PdCl_2$ at pH = 12 (24 h). After a vacuum evaporation of the solvent, the catalyst was dried out at 70 °C for 12 h. Then, the catalyst was reduced with H_2 (20 mL/min) at 250 °C for 1 h.

Pd-Mn/Al_2O_3 samples were prepared by a wet impregnation of the reduced Pd/Al_2O_3 sample with a cymantrene solution in *n*-hexane. After the vacuum evaporation of the solvent, the samples

were treated in an H_2 flow (20 mL/min) at 250–350 °C for 1 h. The effluent gas was analyzed with a quadrupole mass spectrometer QMS-200 (Stanford Research Systems, Sunnyvale, CA, USA).

3.3. Catalyst Characterization

The BET surface area was measured using Gemini VII (Micromeritics Instrument Corp.; Norcross, GA, USA). The samples were degassed at 150 °C for 3 h. The specific surface area was calculated using the BET model for adsorption data in the range of relative pressures P/P_0 = 0.05–0.30.

The metal content of the samples was measured by atomic absorption spectrometry (Perkin-Elmer-AAS, Waltham, MA, USA).

Pulse chemisorption of H_2 and TPD-H_2 was performed by AutoChem 2950HP (Micromeritics Instrument Corp.; Norcross, GA, USA). The samples were preliminarily reduced with H_2 at 250 °C for 1 h, purged with Ar for 30 min and cooled down to 35 °C. The pulse chemisorption was performed with a mixture 10% H_2 + Ar (balance), with a pulse volume of 0.5 mL, in an Ar flow (40 mL/min). TPD-H_2 was performed in an Ar flow (40 mL/min) at a heating rate of 30 K/min to 250 °C.

Transmission electron microscopy (TEM) analysis was carried out using a JEOL JEM-2100 microscope (Jeol Ltd.; Tokyo, Japan) with a 200 kV electron beam energy-dispersive X-ray analyzer (EDX). The mapping of the elements was carried out by scanning transmission electron microscopy (STEM). The samples were milled in an Eppendorf with a glass rod and ultrasonically suspended in isopropanol.

Phase analysis was performed using X-ray powder diffractometer BrukerD2 (Billerica, MA, USA), Cu Kα (λ = 1.5406 Å), 2θ values varied from 5° to 80°.

Diffuse reflectance infrared Fourier transform spectroscopy was done using a NICOLET Protégé 460 (Nicolet, Madison, WI, USA) in the range of 6000–400 cm^{-1} at a resolution of 4 cm^{-1}. For each sample, 500 spectra were recorded to get a good signal-noise ratio. CaF_2 was used as a standard. The spectra were processed with OMNIC software.

3.4. Catalystic Tests

Acetylene hydrogenation was performed in a quartz reactor at atmospheric pressure using AutoChem 2950HP (Micromeritics Instrument Corp.; Norcross, GA, USA). At a given temperature, the flow rate of the reaction mixture was changed to get various values of conversion and selectivity. The contact time was in the range of 0.26–1.81 s^{-1}, the reaction temperature was in the range of 30–50 ºC.

A mixture of 1.94%H_2 + 1.05%C_2H_2 + 5.01%C_2H_4 + Ar (balance) was used as a modeling feed preliminarily prepared in a cylinder. The effluent gas was analyzed online using a quadrupole mass spectrometer QMS-200 (Stanford Research Systems, Sunnyvale, CA, USA) and off-line using FID and TCD detectors in a GC experimental laboratory chromatograph (Gubkin University—Chromos, on the basis of GC-1000 model, Moscow—Dzerjinsk, Russia) using a packed column with HyeSep N. At given operating conditions (temperature, flow rate), the effluent gas was analyzed three times and the final concentration was calculated as the mean value of the three analyses. The carbon balance was closed within 4%.

The acetylene conversion was calculated by the equation:

$$X = \frac{C^{in}_{C2H2} - C^{out}_{C2H2}}{C^{in}_{C2H2}} \times 100\% \quad (3)$$

and ethylene selectivity by:

$$S_{C2H4} = \frac{C^{out}_{C2H4} - C^{in}_{C2H4}}{C^{in}_{C2H2} - C^{out}_{C2H2}} \times 100\% \quad (4)$$

4. Conclusions

A number of Pd-Mn/Al_2O_3 catalysts were designed by the decomposition of cymantrene on reduced Pd/Al_2O_3 in an H_2 atmosphere. The formation of bimetallic catalysts was studied by mass spectrometry analysis of the decomposition products. It was found that the decomposition of cymantrene takes place with hydrogenation of cyclopentadienyl ligands to cyclopentene and cyclopentane, and CO ligands are partially removed by conversion to methane. The catalysts are characterized using N_2 adsorption, H_2 pulse chemisorption, TPD-H_2, TEM, EDX, XRD, and DRIFT spectroscopy. Using the organic precursor—cymantrene provides a high and uniform distribution of Mn over Pd. The addition of manganese changes the H_2 chemisorption and desorption properties of the catalyst: the Pd-Mn/Al_2O_3 samples have shown either a strong chemisorption of H_2 or an insignificant H_2 chemisorption. At the same time, unsaturated C_2 hydrocarbons are strongly chemisorbed on Pd-Mn/Al_2O_3 samples and cannot be removed even under vacuum treatment at elevated temperature. Catalytic tests of the novel Pd-Mn/Al_2O_3 catalysts in hydrogenation of acetylene have shown a higher activity and selectivity thereof to ethylene (up to 20% higher) compared to the non-promoted Pd/Al_2O_3 catalyst. The optimal Mn/Pd ratio and treatment temperature are found. The overall reaction order by reagents is zero for all catalysts, but modification with Mn changes the reaction route from a consecutive pathway for Pd/Al_2O_3 to a parallel one for Pd-Mn/Al_2O_3 catalysts.

Supplementary Materials: The following are available online at http://www.mdpi.com/2073-4344/10/6/624/s1, Figure S1: Peaks of m/z in decomposition of cymantrene in H_2.

Author Contributions: Conceptualization, V.S., D.M.; methodology, D.M., E.S.; software, V.L., E.I., M.K.; validation, A.G., V.S.; formal analysis, V.V., D.M.; resources, V.V., A.G.; data curation, D.M., V.S., E.S., M.K.; writing—original draft preparation, D.M., V.S.; writing—review and editing, D.M., V.S., A.G.; visualization, D.M., V.L.; supervision, V.V., V.S.; project administration, V.V.; funding acquisition, A.G., E.I. All authors have read and agreed to the published version of the manuscript.

Funding: This work was financially supported by the Ministry of Science and Higher Education of the Russian Federation in the part of the analysis technique development in Gubkin University (experimental laboratory gas chromatograph, analysis of hydrocarbons and hydrogen, agreement number 075-11-2019-037 (agreement number between Gubkin University and LLC "Chromos Engineering" 555-19) and as a part of the state task of Gubkin University (synthesis of catalysts, catalytic and phys-chem experiments), project number FSZE-2020-0007 (0768-2020-0007, A.G., E.I., V.V.).

Acknowledgments: The authors thank Olga P. Tkachenko (N.D. Zelinsky Institute of Organic Chemistry) for DRIFT spectra measurements and interpretation. A.G., E.I., V.S., D.M. and V.V. thank LLC "Chromos Engineering" and Andrei Pakhomov.

Conflicts of Interest: The authors declare no conflict of interest.

References

1. Arnold, H.; Döbert, F.; Gaube, J. Hydrogenation reactions. In *Handbook of Heterogeneous Catalysis*, 2nd ed.; Ertl, G., Knözinger, H., Schüth, F., Weitkamp, J., Eds.; Wiley-VCH Verlag GmbH&Co. KGaA: Weinheim, Germany, 2008; Volume 7, pp. 3266–3359.
2. Stytsenko, V.D.; Mel'nikov, D.P. Selective Hydrogenation of Diene and Acetylene Compounds on Metal-Containing Catalysts. *Russ. J. Phys. Chem. A* **2016**, *90*, 932–942. [CrossRef]
3. Huang, D.C.; Chang, K.H.; Pong, W.F.; Tseng, P.K.; Hung, K.J.; Huang, W.F. Effect of Ag-promotion on Pd catalysts by XANES. *Catal. Lett.* **1998**, *53*, 155–159. [CrossRef]
4. Zhang, Q.; Li, J.; Liu, X.; Zhu, Q. Synergetic effect of Pd and Ag dispersed on Al_2O_3 in the selective hydrogenation of acetylene. *Appl. Catal. A Gen.* **2000**, *197*, 221–228. [CrossRef]
5. Pei, G.X.; Liu, X.Y.; Wang, A.; Lee, A.F.; Isaacs, M.A.; Li, L.; Pan, X.; Yang, X.; Wang, X.; Tai, Z.; et al. Ag alloyed Pd single-atom catalysts for efficient selective hydrogenation of acetylene to ethylene in excess ethylene. *Acs Catal.* **2015**, *5*, 3717–3725. [CrossRef]
6. Zhang, Y.; Diao, W.; Williams, C.T.; Monnier, J.R. Selective hydrogenation of acetylene in excess ethylene using Ag- and Au-Pd/SiO_2 bimetallic catalysts prepared by electroless deposition. *Appl. Catal. A Gen.* **2014**, *469*, 419–426. [CrossRef]

7. Zhang, Y.; Diao, W.; Monnier, J.R.; Williams, C.T. Pd-Ag/SiO_2 bimetallic catalysts prepared by galvanic displacement for selective hydrogenation of acetylene in excess ethylene. *Catal. Sci. Technol.* **2015**, *5*, 4123–4132. [CrossRef]
8. Kuhn, M.; Lucas, M.; Claus, P. Long-time stability vs deactivation of Pd-Ag/Al_2O_3 egg-shell catalysts in selective hydrogenation of acetylene. *Ind. Eng. Chem. Res.* **2015**, *54*, 6683–6691. [CrossRef]
9. Ahn, I.Y.; Lee, J.H.; Kim, S.K.; Moon, S.H. Three-stage deactivation of Pd/SiO_2 and Pd-Ag/SiO_2. *Appl. Catal. A Gen.* **2009**, *360*, 38–42. [CrossRef]
10. Shin, E.W.; Choi, C.H.; Chang, K.S.; Na, Y.H.; Moon, S.H. Properties of Si-modified Pd catalyst for selective hydrogenation of acetylene. *Catal. Today* **1998**, *44*, 137–143. [CrossRef]
11. Osswald, J.; Giedigkeit, R.; Jentoft, R.E.; Armbrüster, M.; Girgsdies, F.; Kovnir, K.; Ressler, T.; Grin, Y.; Schlögl, R. Palladium–gallium intermetallic compounds for the selective hydrogenation of acetylene: Part I: Preparation and structural investigation under reaction conditions. *J. Catal.* **2008**, *258*, 210–218. [CrossRef]
12. Osswald, J.; Kovnir, K.; Armbrüster, M.; Giedigkeit, R.; Jentoft, R.E.; Wild, U.; Grin, Y.; Schlögl, R. Palladium-gallium intermetallic compounds for the selective hydrogenation of acetylene: Part II: Surface characterization and catalytic performance. *J. Catal.* **2008**, *258*, 219–227. [CrossRef]
13. Armbrüster, M.; Kovnir, K.; Behrens, M.; Teschner, D.; Grin, Y.; Schlögl, R. Pd-Ga intermetallic compounds as highly selective semihydrogenation catalysts. *J. Am. Chem. Soc.* **2010**, *132*, 14745–14747. [CrossRef] [PubMed]
14. Esmaeili, E.; Rashidi, A.M.; Khodadadi, A.A.; Mortazavi, Y.; Rashidzadeh, M. Palladium-Tin nanocatalyst in high concentration acetylene hydrogenation: A novel deactivation mechanism. *Fuel Process. Technol.* **2014**, *120*, 112–122. [CrossRef]
15. Kim, S.K.; Lee, J.H.; Ahn, I.Y.; Kim, W.J.; Moon, S.H. Performance of Cu-promoted Pd catalysts prepared by adding Cu using a surface redox method in acetylene hydrogenation. *Appl. Catal. A Gen.* **2011**, *401*, 12–19. [CrossRef]
16. Cao, X.; Mirjalili, A.; Wheeler, J.; Xie, W.; Jang, B.W.L. Investigation of the preparation methodologies of Pd-Cu single atom alloy catalysts for selective hydrogenation of acetylene. *Front. Chem. Sci. Eng.* **2015**, *9*, 442–449. [CrossRef]
17. Studt, F.; Abild-Pedersen, F.; Bligaard, T.; Sørensen, R.Z.; Christensen, C.H.; Nørskov, J.K. Identification of non-precious metal alloy catalysts for selective hydrogenation of acetylene. *Science* **2008**, *320*, 1320–1322. [CrossRef]
18. McCue, A.J.; Guerrero-Ruiz, A.; Ramirez-Barria, C.; Rodríguez-Ramos, I.; Anderson, J.A. Selective hydrogenation of mixed alkyne/alkene streams at elevated pressure over a palladium sulfide catalyst. *J. Catal.* **2017**, *355*, 40–52. [CrossRef]
19. McCue, A.J.; McRitchi, C.J.; Shepherd, A.M.; Anderson, J.A. Cu/Al_2O_3 catalysts modified with Pd for selective acetylene hydrogenation. *J. Catal.* **2014**, *319*, 127–135. [CrossRef]
20. Chinayon, S.; Mekasuwandumrong, O.; Praserthdam, P.; Panpranot, J. Selective hydrogenation of acetylene over Pd catalysts supported on nanocrystalline α-Al_2O_3 and Zn-modified α-Al_2O_3. *Catal. Commun.* **2008**, *9*, 2297–2302. [CrossRef]
21. Mashkovsky, I.S.; Baeva, G.N.; Stakheev, A.Y.; Vargaftik, M.N.; Kozitsyna, N.Y.; Moiseev, I.I. Novel Pd-Zn/C catalyst for selective alkyne hydrogenation: Evidence for the formation of Pd-Zn bimetallic alloy particles. *Mendeleev Commun.* **2014**, *24*, 355–357. [CrossRef]
22. Stytsenko, V.D.; Mel'nikov, D.P.; Tkachenko, O.P.; Savel'eva, E.V.; Semenov, A.P.; Kustov, L.M. Selective Hydrogenation of Acetylene and Physicochemical Properties of Pd-Fe/Al_2O_3 Bimetallic Catalysts. *Russ. J. Phys. Chem. A* **2018**, *92*, 862–869. [CrossRef]
23. Jia, J.; Haraki, K.; Kondo, J.N.; Domen, K.; Tamaru, K. Selective hydrogenation of acetylene over Au/Al_2O_3 catalyst. *J. Phys. Chem. B* **2000**, *104*, 11153–11156. [CrossRef]
24. Choudhary, T.V.; Sivadinarayana, C.; Datye, A.K.; Kumar, D.; Goodman, D.W. Acetylene hydrogenation on Au-based catalysts. *Catal. Lett.* **2003**, *86*, 1–8. [CrossRef]
25. Cao, Y.; Sui, Z.; Zhu, Y.; Zhou, X.; Chen, D. Selective Hydrogenation of Acetylene over Pd-In/Al_2O_3 Catalyst: Promotional Effect of Indium and Composition-Dependent Performance. *ACS Catal.* **2017**, *7*, 7835–7846. [CrossRef]

26. Spanjers, C.S.; Held, J.T.; Jones, M.J.; Stanley, D.D.; Sim, R.S.; Janik, M.J.; Rioux, R.M. Zinc inclusion to heterogeneous nickel catalysts reduces oligomerization during the semi-hydrogenation of acetylene. *J. Catal.* **2014**, *316*, 164–173. [CrossRef]
27. Tkachenko, O.P.; Stakheev, A.Y.; Kustov, L.M.; Mashkovsky, I.V.; van den Berg, M.; Grünert, W.; Kozitsyna, N.Y.; Dobrokhotova, Z.V.; Zhilov, V.I.; Nefedov, S.E.; et al. An easy way to Pd-Zn nanoalloy with defined composition from a heterometallic Pd(μ-OOCMe)$_4$Zn(OH$_2$) complex as evidenced by XAFS and XRD. *Catal. Lett.* **2006**, *112*, 155–161. [CrossRef]
28. Vinokurov, V.A.; Stavitskaya, A.V.; Chudakov, Y.A.; Glotov, A.P.; Ivanov, E.V.; Gushchin, P.A.; Lvov, Y.M.; Maximov, A.L.; Muradov, A.V.; Karakhanov, E.A. Core-shell nanoarchitecture; Schiff-base assisted synthesis of ruthenium in clay nanotubes. *Pure Appl. Chem.* **2018**, *90*, 825–832. [CrossRef]
29. Vinokurov, V.A.; Stavitskaya, A.V.; Glotov, A.P.; Novikov, A.A.; Zolotukhina, A.V.; Kotelev, M.S.; Gushchin, P.A.; Ivanov, E.V.; Darrat, Y.; Lvov, Y.M. Nanoparticles Formed onto/into Halloysite Clay Tubules: Architectural Synthesis and Applications. *Chem. Rec.* **2018**, *18*, 858–867. [CrossRef]
30. Vinokurov, V.; Glotov, A.; Chudakov, Y.; Stavitskaya, A.; Ivanov, E.; Gushchin, P.; Zolotukhina, A.; Maximov, A.; Karakhanov, E.; Lvov, Y. Core/Shell Ruthenium–Halloysite Nanocatalysts for Hydrogenation of Phenol. *Ind. Eng. Chem. Res.* **2017**, *56*, 14043–14052. [CrossRef]
31. Glotov, A.; Levshakov, N.; Stavitskaya, A.; Artemova, M.; Gushchin, P.; Ivanov, E.; Vinokurov, V.; Lvov, Y. Templated Self-Assembly of Ordered Mesoporous Silica on Clay Nanotubes. *Chem. Commun.* **2019**, *55*, 5507–5510. [CrossRef]
32. Kang, J.H.; Shin, E.W.; Kim, W.J.; Park, J.D.; Moon, S.H. Selective hydrogenation of acetylene on Pd/SiO$_2$ catalysts promoted with Ti, Nb and Ce oxides. *Catal. Today* **2000**, *63*, 183–188. [CrossRef]
33. Kang, J.H.; Shin, E.W.; Kim, W.J.; Park, J.D.; Moon, S.H. Selective hydrogenation of acetylene on TiO$_2$-added Pd catalysts. *J. Catal.* **2002**, *208*, 310–320. [CrossRef]
34. Gulyaeva, Y.K.; Kaichev, V.V.; Zaikovskii, V.I.; Kovalyov, E.V.; Suknev, A.P.; Bal'zhinimaev, B.S. Selective hydrogenation of acetylene over novel Pd/fiberglass catalysts. *Catal. Today* **2015**, *245*, 139–146. [CrossRef]
35. Gulyaeva, Y.K.; Kaichev, V.V.; Zaikovskii, V.I.; Suknev, A.P.; Bal'zhinimaev, B.S. Selective hydrogenation of acetylene over Pd/Fiberglass catalysts: Kinetic and isotopic studies. *Appl. Catal. A Gen.* **2015**, *506*, 197–205. [CrossRef]
36. Shesterkina, A.A.; Kozlova, L.M.; Kirichenko, O.A.; Kapustin, G.I.; Mishin, I.V.; Kustov, L.M. Influence of the thermal treatment conditions and composition of bimetallic catalysts Fe-Pd/SiO$_2$ on the catalytic properties in phenylacetylene hydrogenation. *Russ. Chem. Bull.* **2016**, *65*, 432–439. [CrossRef]
37. Shesterkina, A.A.; Kozlova, L.M.; Mishin, I.V.; Tkachenko, O.P.; Kapustin, G.I.; Zakharov, V.P.; Vlaskin, M.S.; Zhuk, A.Z.; Kirichenko, O.A.; Kustov, L.M. Novel Fe-Pd/γ-Al2O3 catalysts for the selective hydrogenation of C≡C bonds under mild conditions. *Mendeleev Commun.* **2019**, *29*, 339–342. [CrossRef]
38. Rozovskii, A.Y.; Stytsenko, V.D.; Nizova, S.A.; Belov, P.S.; Dyakonov, A.Y. Catalyst for dehydrogenation of oxygen containing dervatives of the cyclohexane series into corresponding cyclic ketones and/or phenols. U.S. Patent 4,363,750, 14 December 1982.
39. Rozovskii, A.Y.; Stytsenko, V.D.; Nizova, S.A.; Belov, P.S.; Dyakonov, A.Y. Catalyst for dehydrogenation oxygen-containing dervatives of the cyclohexane series into the corresponding cyclic ketones and/or phenols. U.S. Patent 4,415,477, 15 November 1983.
40. Rozovskii, A.Y.; Stytsenko, V.D.; Nizova, S.A.; Belov, P.S.; Dyakonov, A.Y. Catalyst and process for dehydrogenation of oxygen-containing dervatives of the cyclohexane series into corresponding cyclic ketones and/orphenols. U.S. Patent 4,417,076, 22 November 1983.
41. Stytsenko, V.D. Surface modified bimetallic catalysts: Preparation, characterization, and applications. *Appl. Catal. A* **1995**, *126*, 1–26. [CrossRef]
42. Agnelli, M.; Louessard, P.; El Mansour, A.; Candy, J.P.; Bournonville, J.P.; Basset, J.M. Surface organometallic chemistry on metals preparation of new selective bimetallic catalysts by reaction of tetra-n-butyl tin with silica supported Rh, Ru and Ni. *Catal. Today* **1989**, *6*, 63–72. [CrossRef]
43. Adúriz, H.R.; Gígola, C.E.; Sica, A.M.; Volpe, M.A.; Touroude, R. Preparation and characterization of Pd-Pb catalysts for selective hydrogenation. *Catal. Today* **1992**, *15*, 459–467. [CrossRef]
44. Glotov, A.; Stytsenko, V.; Artemova, M.; Kotelev, M.; Ivanov, E.; Gushchin, P.; Vinokurov, V. Hydroconversion of Aromatic Hydrocarbons over Bimetallic Catalysts. *Catalysts* **2019**, *9*, 384. [CrossRef]
45. NIST Chemistry WebBook. Available online: https://webbook.nist.gov (accessed on 10 April 2020).

46. Wang, S.Y.; Moon, S.H.; Vannice, M.A. The Effect of SMSI (Strong Metal-Support Interaction) Behavior on CO Adsorption and Hydrogenation on Pd Catalysts. *J. Catal.* **1981**, *71*, 167–174. [CrossRef]
47. Lee, J.H.; Kim, S.K.; Ahn, I.Y.; Kim, W.J.; Moon, S.H. Performance of Ni-added Pd-Ag/Al_2O_3 catalysts in the selective hydrogenation of acetylene. *Korean J. Chem. Eng.* **2012**, *29*, 169–172. [CrossRef]
48. Li, Z.Y.; Liu, Z.L.; Liang, J.C.; Xu, C.W.; Lu, X. Facile synthesis of Pd-Mn_3O_4/C as high efficient electrocatalyst for oxygen evolution reaction. *J. Mater. Chem. A* **2014**, *2*, 18236–18240. [CrossRef]
49. Romano, C.A.; Zhou, M.; Song, Y.; Wysocki, V.H.; Dohnalkova, A.C.; Kovarik, L.; Paša-Tolić, L.; Tebo, B.M. Biogenic manganese oxide nanoparticle formation by a multimeric multicopper oxidase Mnx. *Nat. Commun.* **2017**, *8*, 1–8. [CrossRef] [PubMed]
50. Yasmin, S.; Cho, S.; Jeon, S. Electrochemically reduced grapheme-oxide supported bimetallic nanoparticles highly efficient for oxygen reduction reaction with excellent methanol tolerance. *Appl. Surf. Sci.* **2018**, *434*, 905–912. [CrossRef]
51. Wang, W.; Yuan, F.; Niu, X.; Zhu, Y. Preparation of Pd supported on La(Sr)-Mn-O Perovskite by microwave Irradiation Method and Its Catalytic Performances for the Methane Combustion. *Sci. Rep.* **2016**, *6*, 19511. [CrossRef]
52. Kustov, L.M. New trends in IR-spectroscopic characterization of acid and basic sites in zeolites and oxide catalysts. *Top. Catal.* **1997**, *4*, 131–144. [CrossRef]
53. Merck Webpage. Available online: https://www.sigmaaldrich.com/technical-documents/articles/biology/ir-spectrum-table.html (accessed on 18 May 2020).
54. Lapinski, M.P.; Ekerdt, J.G. Infrared Identification of Adsorbed Surface Species on Ni/SiO_2 and Ni/Al_2O_3 form Ethylene and Acetylene Adsorption. *J. Phys. Chem.* **1990**, *94*, 4599–4610. [CrossRef]
55. Urmès, C.; Schweitzer, J.M.; Cabiac, C.; Schuurman, Y. Kinetic Study of the Selective Hydrogenation of Acetylene over Supported Palladium under Tail-End Conditions. *Catalysts* **2019**, *9*, 180. [CrossRef]
56. Insorn, P.; Kitiyanan, B. Selective hydrogenation of mixed C_4 containing high vinyl acetylene by Mn-Pd, Ni-Pd and Ag-Pd on Al_2O_3 catalysts. *Catal. Today* **2015**, *256*, 223–230. [CrossRef]